ISSN No:-2456-2165 https://doi.org/10.38124/ijisrt/26aug944

Reservoir-Scale Caprock Seal Integrity for CO_2 and Hydrogen Storage: A Critical Review of Upscaling Methods and Uncertainty Propagation

Raymond Oluwadolapo Aderoju[1]; Mojibola Esther Afolabi[2]; Joy Ojodunwene Onuh[3]

[1]Geology Department, University of Georgia, Athens, USA
[2]Department of Geology, Portland State University, Oregon, UGA
[3]Department of Civil and Environmental Engineering, University of Vermont, Vermont, USA

Publication Date: 2026/09/01

Abstract: Reservoir-scale caprock seal integrity during geological CO_2 and underground hydrogen storage (UHS) depends on processes occurring well below the scale at which a safety assessment typically treats mineral dissolution and precipitation, capillary entry pressure at grain contacts, and stress-dependent pore structure. This review addresses one question precisely: how is finer-scale hydromechanical alteration translated into defensible continuum-scale parameters and reservoir-scale predictions, and what information is lost in that translation? We distinguish pore-scale observation, core-scale measurement, constitutive closure, and reservoir-scale prediction as categorically different evidence types rather than treating them as interchangeable. Published experimental and simulation studies consistently document localized, order-of-magnitude permeability increases along preferential dissolution pathways at small scale; the small number of studies that have attempted the full upscaling chain against an actual site report comparatively small net bulk change over decades to a century. We treat this as an open scale-dependence problem rather than a resolved discrepancy, and evaluate candidate explanations, including volume averaging, mineral buffering, connectivity and percolation thresholds, and flow-regime dependence via the Damköhler and Peclet numbers, against what published evidence demonstrates versus what remains a hypothesis. CO_2 and H_2 are treated as physically distinct problems, compared on molecular size, interfacial tension, capillary entry pressure, and reactivity, before their reservoir-scale outcomes are compared. We propose a physics-consistent workflow connecting characterization to reservoir-scale seal-integrity prediction with explicit uncertainty propagation and identify where physics-informed machine learning could prospectively, not presently, contribute. Claims not supported by verified evidence are flagged explicitly rather than filled with plausible-sounding literature.

Keywords: *Caprock Integrity; Reservoir-Scale Upscaling; Seal Integrity Assessment; Representative Elementary Volume; Uncertainty Propagation; Carbon Storage; Underground Hydrogen Storage*.

How to Cite: Raymond Oluwadolapo Aderoju; Mojibola Esther Afolabi; Joy Ojodunwene Onuh (2026) Reservoir-Scale Caprock Seal Integrity for CO_2 and Hydrogen Storage: A Critical Review of Upscaling Methods and Uncertainty Propagation. *International Journal of Innovative Science and Research Technology*, 11(8), 2291-2303. https://doi.org/10.38124/ijisrt/26aug944

I. INTRODUCTION

Geological carbon storage (GCS) and underground hydrogen storage (UHS) both require that an injected fluid remain trapped beneath a caprock for periods ranging from decades for cyclic UHS operation to centuries for permanent CO_2 sequestration. Containment is not a single property but the joint outcome of four distinct mechanisms: capillary sealing, in which the buoyant fluid cannot displace brine from the caprock pore network until the capillary entry pressure is exceeded; hydraulic sealing, in which the caprock's intrinsic permeability limits advective flux even where capillary entry has occurred; geochemical alteration, in which dissolution or precipitation reactions change pore structure and therefore affect both of the above over time; and mechanical integrity, in which pore-pressure perturbation changes effective stress [14] and can open new flow paths through fracturing or fault reactivation [13]. Each mechanism operates over a different characteristic length scale, from the nanometer-to-micrometer scale of a clay pore throat governing capillary entry pressure to the kilometer scale of the caprock formation a regulator must certify as intact.

➢ *Highlights*

- Pore-scale, core-scale, constitutive closure, and reservoir-scale evidence are treated as distinct, non-interchangeable classes.

ISSN No:-2456-2165 https://doi.org/10.38124/ijisrt/26aug944

- Pore-scale permeability increases by orders of magnitude, but reservoir-scale studies report only 3- 4% net change; this remains an open, unresolved gap.
- A representative elementary volume may not exist for heterogeneous caprock, so averaging can discard the pathway information that controls leakage.
- CO_2 and H_2 are compared via the Damköhler, Péclet, and capillary numbers, showing the two gases occupy different pore-scale flow-reaction regimes.
- Five uncertainty categories are traced from pore to reservoir; structural uncertainty in closure choice is least constrained, as no reviewed study tested alternative closures.
- CNN, GNN, and physics-informed ML are reviewed as prospective, not present; none has been validated on caprock-specific reactive, multiphase behavior.

This scale gap is the central technical obstacle. Direct pore-resolving simulation, whether pore-network modeling [1] or Lattice Boltzmann and Navier-Stokes solvers on segmented micro-CT geometry [3], can resolve individual reaction and flow events but cannot be extended computationally to a reservoir-scale domain; a single core plug already represents a substantial simulation, and a caprock formation is many orders of magnitude larger. Continuum reservoir simulators, conversely, operate on effective parameters, such as permeability, porosity, relative permeability, and capillary pressure, that must be supplied through a closure relationship rather than derived pore-by-pore [17]. Naive transfer of a pore-scale rate constant or dissolution pattern directly into a reservoir-scale grid cell, without an explicit upscaling step, risks either propagating a highly localized, non-representative value across an entire grid block or averaging away the specific preferential pathways that would control leakage.

The cross-scale character of the CO_2 storage problem specifically, spanning pore-scale reaction to regional-scale reservoir management, has been recognized explicitly in the literature [2], but previous reviews have substantially advanced the two ends of this problem separately. Digital rock physics and pore-network Modeling reviews have matured the pore-scale characterization and simulation toolkit. Reservoir-scale reactive-transport and geomechanical reviews have matured continuum-scale caprock assessment. What has received comparatively little synthesis is the transition itself: which pore-scale quantities survive upscaling intact, which are averaged into an effective parameter, and which are lost outright unless explicitly reintroduced through sub-grid parameterization. This review's contribution relative to those two, largely separate literatures is the explicit treatment of that transition as the primary object of study, not as a brief bridging paragraph between otherwise independent bodies of work, formalized through the input-transformation-output-uncertainty structure developed in Section 2.

We ask four questions. RQ1: Which pore-scale and core-scale hydromechanical degradation mechanisms are directly demonstrated by published experiments or simulations, as opposed to inferred or assumed? RQ2: Through what upscaling methods- volume averaging, representative elementary volume analysis, empirical constitutive closure- are pore-scale observations converted into reservoir-scale parameters, and what uncertainty does each step introduce? RQ3: Among the small number of studies that have attempted the full pore-to-reservoir chain against an actual site, what do they report, and does that support a general conclusion about caprock behaviour or only a site-specific one? RQ4: Which CO_2-derived upscaling concepts can be transferred to H2 storage on physical grounds, and which cannot?

➢ *The Pore-to-Reservoir Scale Transition Problem*

This review organizes its technical content around four categorically distinct evidence types, which are not interchangeable and are kept explicitly separate throughout: pore-scale observation (direct imaging or simulation of individual pores and reactions, typically nanometer to millimeter scale); core-scale measurement (bulk property measurement on a physical sample, typically millimeter to decimeter scale, that already represents an averaged outcome of many pore-scale events); constitutive closure (an empirical or semi-empirical relationship, such as a porosity-permeability power law [17], that stands in for unresolved pore-scale detail at the continuum scale); and reservoir-scale prediction (a continuum simulation output, such as a leakage rate or failure metric, that depends on the closure relationships supplied to it and cannot be independently verified against pore-scale physics without a separate upscaling study).

ISSN No:-2456-2165 https://doi.org/10.38124/ijisrt/26aug944

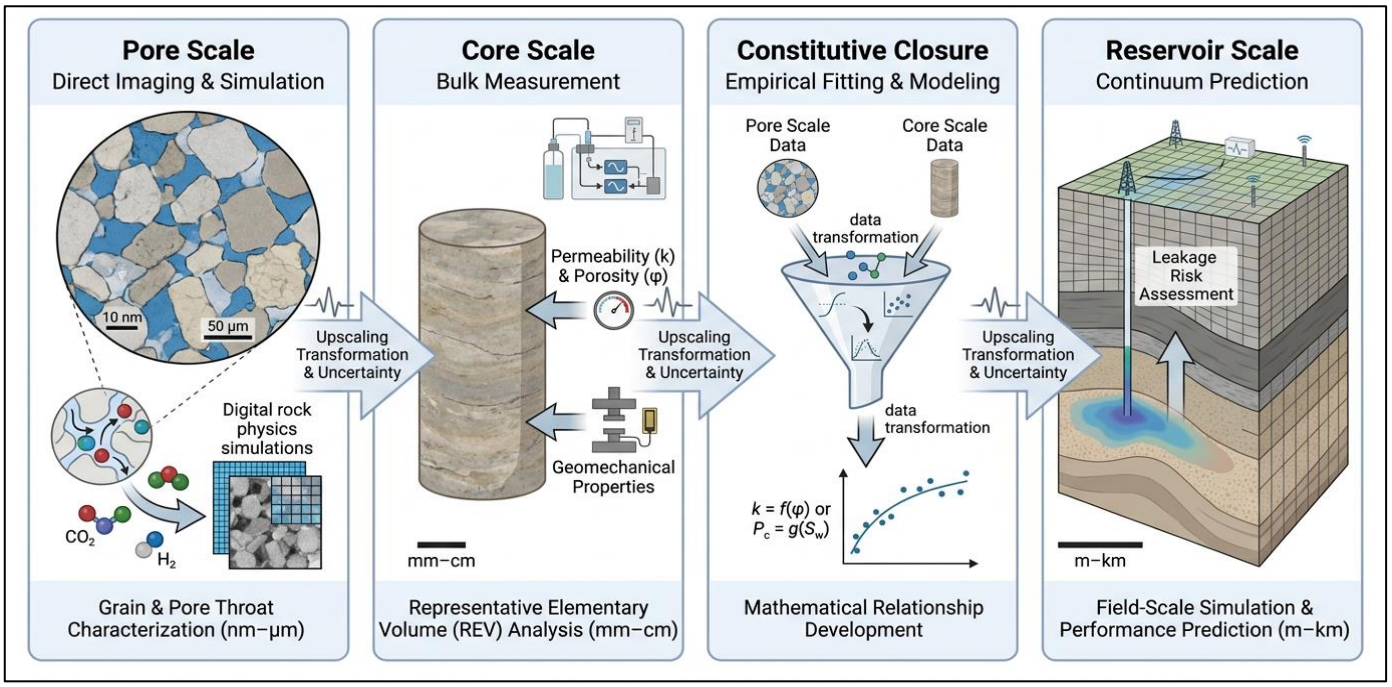

Fig 1 Scale Hierarchy Connecting Pore-Scale Mechanisms to Reservoir-Scale Caprock Outcomes, with the Two Upscaling Transitions this Review Treats as its Central Problem.

Each transition between these categories can be described as an input, an upscaling transformation, an output, and an associated uncertainty. Micro-CT geometry, segmented into pore and solid phases, is transformed by network extraction or direct simulation into pore topology and hydraulic properties, with segmentation and resolution uncertainty attached. Pore-scale flow and reactive-transport simulation is transformed by volume averaging or homogenization into effective permeability, dispersion, and capillary properties, with representative-elementary-volume (REV) uncertainty attached. Core-scale properties are transformed by constitutive relationships into reservoir grid parameters, with spatial scaling uncertainty attached. Reservoir simulation output is transformed by leakage or seal-integrity metrics into an operational risk statement, with structural and parameter uncertainty attached. Sections 3 through 7 examine each transition; Section 7 examines the evidence for how well the full chain has been demonstrated; Section 8 traces how uncertainty accumulates across it.

II. GOVERNING PHYSICS ACROSS SCALES

Pore-scale characterization of caprock lithology, typically via segmented micro-CT imaging and pore-network or direct numerical simulation, provides the geometric basis, pore-throat radius distribution, connectivity, and specific surface area, from which the effective properties used below are computed; that characterization methodology is well established elsewhere [1,3,11,16] and is not re-derived here, since this review's focus is the transition from pore-scale properties to reservoir-scale prediction rather than pore-scale characterization itself. Equations are introduced here only where they clarify what is preserved, and what is lost, in that transition; they are not presented as a general methods catalogue.

- *Pore-Scale Flow: Stokes/Navier-Stokes and Lattice Boltzmann*

At the pore scale, single-phase flow is governed by the Navier-Stokes equations, or, for the low-Reynolds-number regime typical of pore-throat flow, their Stokes-flow limit:

$$\rho\left(\frac{\partial u}{\partial t} + (u\cdot\nabla)u\right) = -\nabla p + \mu\nabla^2 u + F_s$$

Where u is velocity, p is pressure, ρ and μ are density and viscosity, and Fs is an interfacial-tension source term where two fluid phases are present. Directly discretizing this system on segmented pore geometry is computationally expensive at reservoir-relevant sample sizes, which motivates the Lattice Boltzmann method (LBM), most commonly the single-relaxation-time BGK form.

$$f_i(x + e_i\Delta t, t + \Delta t) = f_i(x,t) - (1/\tau)[f_i(x,t) - f_i^{eq}(x,t)]$$

Where fi is the particle distribution along lattice direction i, τ the relaxation time setting kinematic viscosity, and f eq i the local equilibrium distribution, with macroscopic density and momentum recovered by summation over lattice directions. This general pore-scale multiphase simulation framework, and its validation against core-flood experiment, is reviewed comprehensively elsewhere [3]. What is preserved in LBM output is pore-scale flow structure and, from it, digitally computed permeability and relative permeability for the specific sample simulated. What is lost, immediately upon reporting a single effective permeability for that sample, is the spatial distribution of flow within it, information that matters directly for predicting where a preferential pathway would develop under sustained reactive flow.

ISSN No:-2456-2165 https://doi.org/10.38124/ijisrt/26aug944

➢ *Reactive Transport and Mineral Kinetics*

Solute transport is governed by the advection-diffusion-reaction equation, part of a governing-equation structure reviewed comprehensively across pore, meso, and continuum scales elsewhere [18],

$$\frac{\partial C}{\partial t} + \nabla \cdot (uC) = \nabla \cdot (D\nabla C) + R_{rxn}$$

Where C is solute concentration, D the dispersion coefficient, and Rrxn the reaction source/sink term, coupled at mineral surfaces to a kinetic rate law of the general transition-state form.

$$r = k \cdot A \left(1 - \frac{Q}{Keq}\right)$$

With r the dissolution or precipitation rate, k the intrinsic rate constant, A the reactive surface area, and Q/Keq the saturation state. The reactive surface area term is scale-dependent in a way this equation does not itself resolve: A measured on a crushed, high-surface-area powder in a batch experiment is not the same quantity as the geometrically accessible surface area in an intact pore network, and applying a batch-derived k uniformly across a heterogeneous pore-network model has been shown to under-predict the spatial concentration of dissolution into wormholes once local flow velocity and surface area begin to feedback on one another [4,5,6]. What is lost in adopting a single, batch-calibrated k for a continuum-scale grid block is precisely the possibility of that feedback: a reservoir simulator supplied with one uniform rate constant cannot generate a wormhole even if the underlying rock would, which is a structural limitation of the closure in Section 3.4 rather than a numerical error to be refined away.

➢ *Capillary Sealing: the Young-Laplace Relation*

Capillary entry pressure, the pressure difference the buoyant CO_2 or H_2 phase must exceed to displace brine from the largest connected pore throats, is the primary sealing mechanism for a caprock with negligible bulk permeability, and is governed by the Young-Laplace relation,

$$P_{ce} = \frac{2\sigma \cos\theta}{r}$$

Where σ is interfacial tension, θ the contact angle, and r the effective pore-throat radius. Because entry pressure scales inversely with pore-throat radius, a caprock's sealing capacity is controlled disproportionately by its smallest connected throats, precisely the geometric feature most vulnerable to the imaging and segmentation uncertainty discussed in Section 3.1, and most directly altered by the dissolution and precipitation reactions discussed in Section 3.2. A direct comparison of CO_2 and H_2 capillary sealing on a shared caprock proxy, using measured contact angles across a pressure-temperature range relevant to storage conditions, found that entry pressure and gas-column height depend on the same governing relation for both gases but differ substantially in magnitude because of their contrasting interfacial tension with brine [19] (Section 6).

➢ *Effective Stress and Porosity-Permeability Closure*

Stress-driven, as opposed to reaction-driven, pore structure change is governed by the Biot effective-stress relation [14], with a representative closure applied in reservoir-scale caprock assessment taking the empirical form

$$k = k_0 \cdot exp\left(22.2\left(\frac{\phi}{\phi_0}\right) - 22.2\right)$$

Coupled to an effective-stress-dependent porosity relation:

$$\phi = (\phi_0 - \phi_r)\, exp(-5 \times 10^{-8} \cdot \sigma'_M) + \phi_r$$

Where σ′M is the mean effective stress, and ϕr is the residual porosity at high stress [9]. The exponential coupling between permeability and normalized porosity change is a standard geomechanical functional form, consistent with the general treatment of stress-dependent permeability in poroelastic media; the specific numerical constants shown here (22.2, 5×10−8) are fitted to the Farnsworth Morrow shale caprock specifically [9] and are not universal, a distinction the closure literature does not always make explicit when such relations are transferred between sites. This closure, like the porosity-permeability relations reviewed comprehensively for (bio)geochemically altered porous media generally [17], is fitted empirically rather than derived from pore geometry; it is the mechanism by which both reaction-driven and stress-driven porosity change are collapsed into the single permeability field a reservoir simulator actually uses, and both mechanisms are frequently modelled separately rather than coupled in the studies synthesized in Section 3.2.

III. DIMENSIONLESS ANALYSIS AND FLOW-REACTION REGIMES

Whether a given injection scenario reproduces the wormholing behaviour documented at the pore scale, or instead produces diffuse, spatially uniform dissolution, is governed by dimensionless groups rather than by flow rate or reaction rate in isolation. The Peclet number, Pe = uL/D, compares advective to diffusive transport; the Damkohler number, Da = k·a_s·L/u, where a_s is specific reactive surface area per unit pore volume (units of inverse length, distinct from the total reactive surface area A used in the local rate law of Section 3.2), compares reaction rate to transport rate; the capillary number, Ca = μu/σ, compares viscous to interfacial forces and governs multiphase displacement pattern; and the pore-scale Reynolds number, Re = ρuL/μ, confirms whether the Stokes-flow assumption in Section 3.1 is appropriate (Re is small, typically well under 1, for essentially all caprock pore-throat flow, which is why Stokes flow rather than full Navier-Stokes is the standard pore-scale assumption).

ISSN No:-2456-2165 https://doi.org/10.38124/ijisrt/26aug944

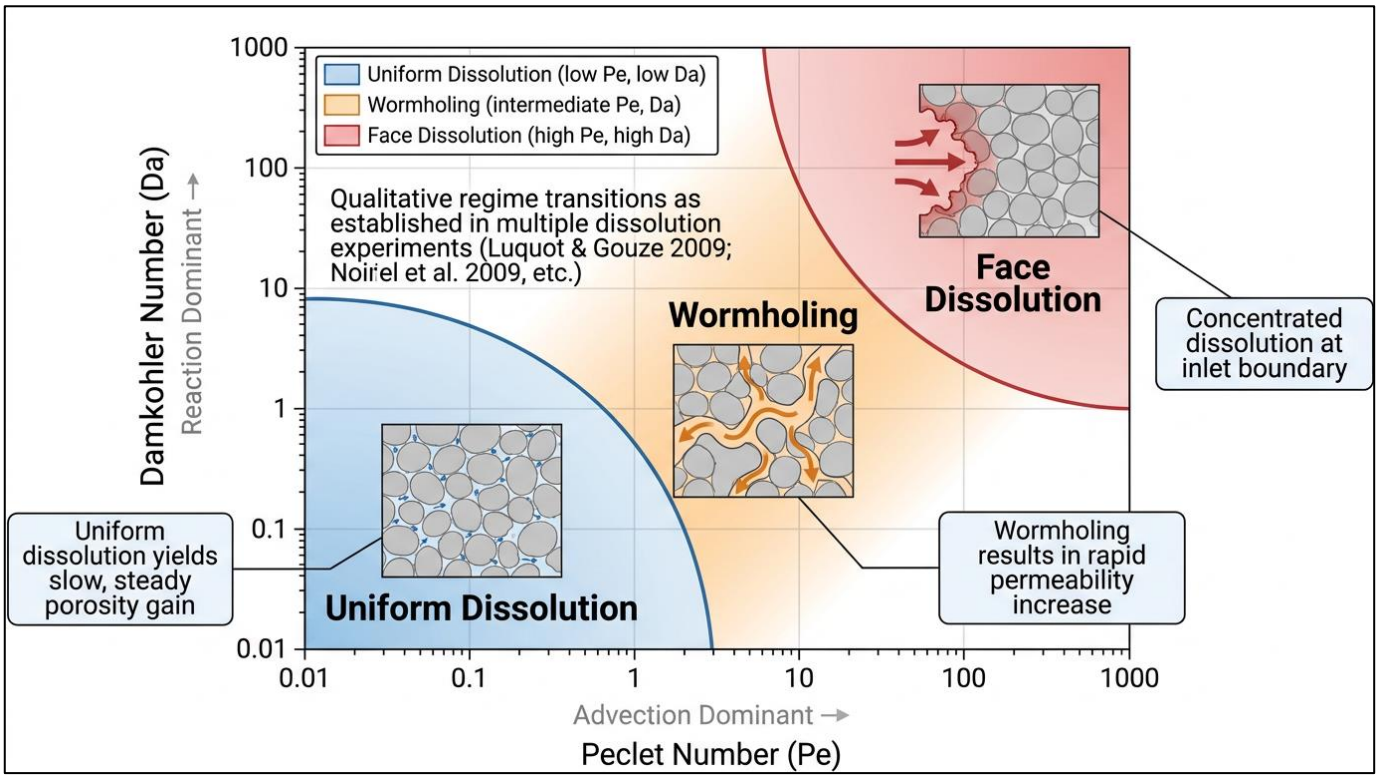

Fig 2 Conceptual Pore-Scale Flow-Reaction Regime Map Using the Damköhler and Peclet Numbers, Illustrating the Qualitative Transition from Face Dissolution to Wormholing to Uniform Dissolution Documented Across Independent Dissolution Experiments.

Independent carbonate dissolution experiments and pore-network simulations consistently report the same qualitative regime sequence: at low Da (reaction slow relative to transport), dissolution is diffuse and porosity increases relatively uniformly; near Da approximately 1, with Pe sufficiently large that advection dominates locally, wormhole channels form and permeability increases most dramatically for a given amount of mineral dissolved; at high Da (reaction fast relative to transport), dissolution concentrates at the inlet face and penetrates the sample only shallowly [6,10]. This regime dependence is directly demonstrated by the cited experiments; the specific numerical Da and Pe boundaries shown in Fig. 2 are illustrative rather than fitted to a reported dataset, since the reviewed reservoir-scale studies did not report the dimensionless numbers characterizing their own simulated conditions, which limits how precisely their outcomes can be located on this regime map.

The properties compared systematically in Section 6 (Fig. 4) place CO_2 and H_2 at different, non-overlapping regions of this dimensionless space for a given injection velocity and pore geometry, rather than merely at different absolute rates of the same process. H_2's viscosity is markedly lower than CO_2's under storage conditions, so at equal flow velocity the capillary number $Ca = \mu u/\sigma$ is smaller for H_2 than for CO_2 through the viscosity term alone; H_2's higher interfacial tension with brine [19] reduces Ca further, placing H_2 displacement more consistently in the capillary-dominated, less fingering-prone regime than CO_2 at comparable injection rates. H_2's higher diffusivity in brine shifts Pe = uL/D downward relative to CO_2 at fixed velocity and length scale, favoring more diffusion-dominated, less advection-localized transport, the opposite direction from the high-Pe conditions identified above as necessary for wormhole formation. Neither comparison has been tested directly against the Da-Pe regime boundaries in Fig. 2, since none of the reviewed pore-scale wormholing studies used H_2 as the reactive fluid [6,10]; pore-scale lattice Boltzmann simulation of H_2-brine multiphase flow has been demonstrated for underground hydrogen storage more generally [32], which confirms the simulation capability exists, but that capability has not yet been directed at the reactive, wormholing-regime question this section raises. The direction of the shift follows directly from the verified property contrasts in Fig. 4, but the magnitude, and whether it moves H_2 systems meaningfully across a regime boundary rather than only along a gradient within the same regime, remains untested by the studies synthesized in this section.

ISSN No:-2456-2165 https://doi.org/10.38124/ijisrt/26aug944

➢ *Representative Elementary Volume and the Loss of Pore-Scale Information*

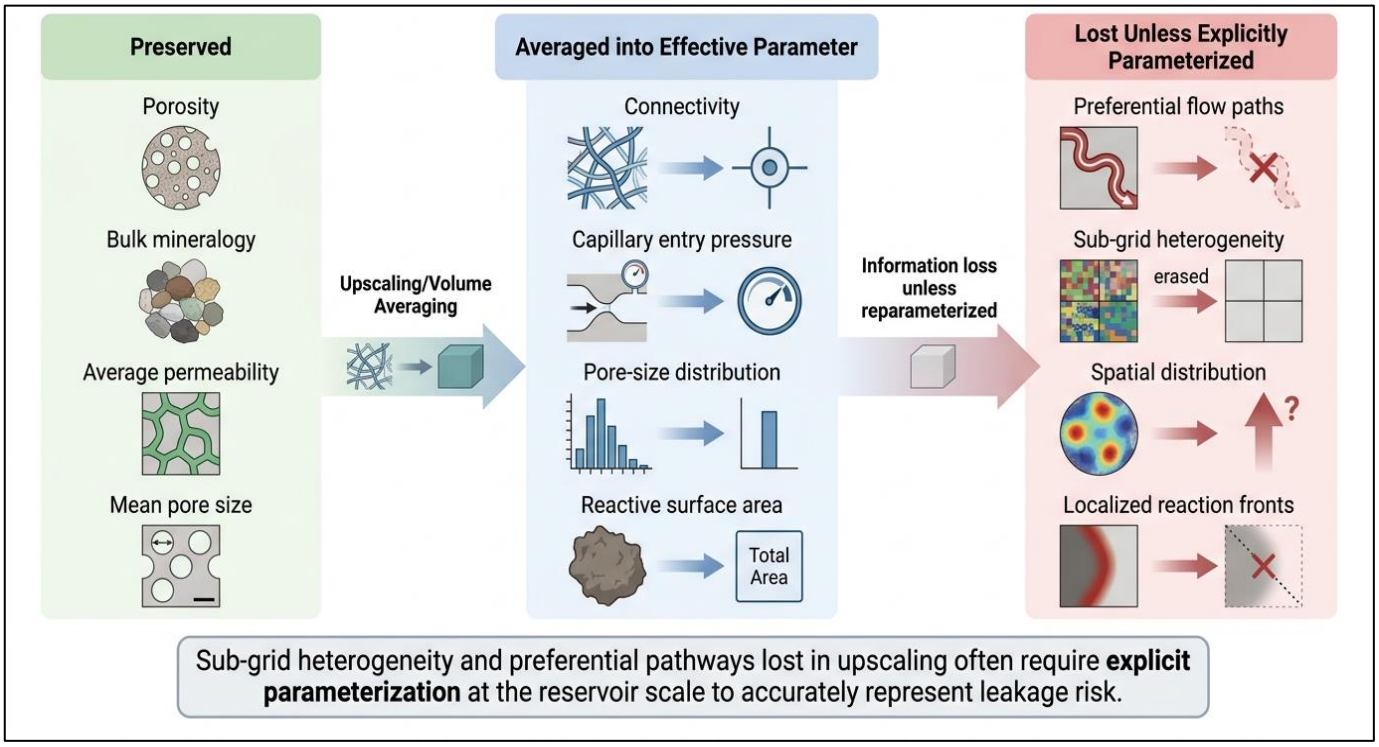

Fig 3 Fate of Representative Pore-Scale Quantities During Transfer to Reservoir/Continuum Scale: Preserved, Homogenized into an Effective Parameter, or Lost Unless Explicitly Reintroduced Through Sub-Grid Parameterization.

A representative elementary volume is the smallest sample or simulation domain at which a property of interest becomes statistically stable; in Bear's original formulation, the volume at which adding or removing a single pore no longer measurably changes the computed property [16]. Two distinct REVs are relevant here and are not the same volume: a geometrical REV, at which porosity and pore-size distribution stabilize, and a transport REV, at which effective permeability or relative permeability stabilizes; the transport REV is generally larger, and its existence is not guaranteed for the same sample size that satisfies the geometrical REV [33, 36]. For relative permeability specifically, recent work has emphasized that the classical REV concept, a volume large enough for spatial variability to average out, becomes increasingly difficult to satisfy as digital core analysis moves toward smaller imaged sub-volumes, precisely the regime much pore-scale caprock imaging operates in [33].

An REV may not exist at any practically imageable scale where heterogeneity is structured rather than random: long-range connected fracture networks, spatially correlated mineralogical layering, or anisotropic bedding-parallel permeability in a shale caprock can all produce a property that continues to change with sample size well beyond what is computationally tractable to image and simulate.

This matters directly for caprock integrity because averaging inherently discards exactly the information, the location and connectivity of a preferential pathway, that controls whether leakage occurs at all; a reservoir grid block reporting a low average permeability can still contain a thin, connected, high-permeability pathway that dominates actual flow, a distinction the REV-averaged value cannot represent by construction unless the sub-grid heterogeneity is separately parameterized [16,17].

➢ *CO_2 versus H_2: Divergent Pore-Scale Physics before Comparison*

CO_2 and H_2 differ on essentially every physical property governing caprock interaction, and these differences are compared here before any comparison of reservoir-scale outcomes is attempted (Fig. 4). H_2 has a smaller molecular diameter and higher diffusivity than CO_2, properties relevant to whether it can access sub-nanopore volume inaccessible to CO_2. H_2 has substantially lower density and viscosity than CO_2 under storage conditions, affecting both buoyant migration rate and multiphase displacement pattern (capillary number, Section 4). Measured directly on a shared caprock proxy, H_2 shows higher interfacial tension with brine than CO_2 across the same pressure-temperature range, which, by the Young-Laplace relation (Section 3.3), implies a higher capillary entry pressure and therefore, all else equal, more favorable capillary sealing, at a given pore-throat radius, than CO_2 [19].

That comparison was made using equilibrium contact angle; contact angle hysteresis, the difference between advancing and receding contact angle that governs snap-off and residual trapping during cyclic displacement, is not established by the source cited above for either gas on a caprock-relevant substrate. Hysteresis is a documented, measurable phenomenon in this general class of system: CO_2 wettability studies on real caprock samples report systematic differences between advancing and receding contact angles

ISSN No:-2456-2165 https://doi.org/10.38124/ijisrt/26aug944

[22], and six-cycle CO_2-H_2O injection experiments on analogue storage reservoir rock show that repeated cycling produces continuously increasing differential pressure attributed to cumulative residual trapping, a direct hysteresis effect at the core scale [23]. Whether the magnitude of this effect, characterized for CO_2, transfers quantitatively to H_2 given the property contrasts in Fig. 4 is not established by either source and is flagged as a gap rather than assumed comparable, particularly given that UHS involves the repeated advancing/receding cycles where hysteresis matters most and CO_2 storage largely does not; the pore-to-continuum-scale treatment of hysteresis itself remains an active methodological question even within the CO_2-only literature [24]. H2's aqueous solubility is markedly lower than CO_2's, limiting the dissolution-driven geochemical pathway that dominates CO_2-caprock interaction (Section 3.2); H_2's caprock reactivity instead proceeds substantially through redox and microbially mediated pathways with no direct CO_2 analogue [20,21]. Operationally, UHS is characterized by cyclic injection and withdrawal on timescales of days to seasons, rather than the effectively continuous injection typical of CO_2 sequestration, which imposes a fatigue-type mechanical loading history on the caprock that the CO_2 literature reviewed in Section 7 does not address.

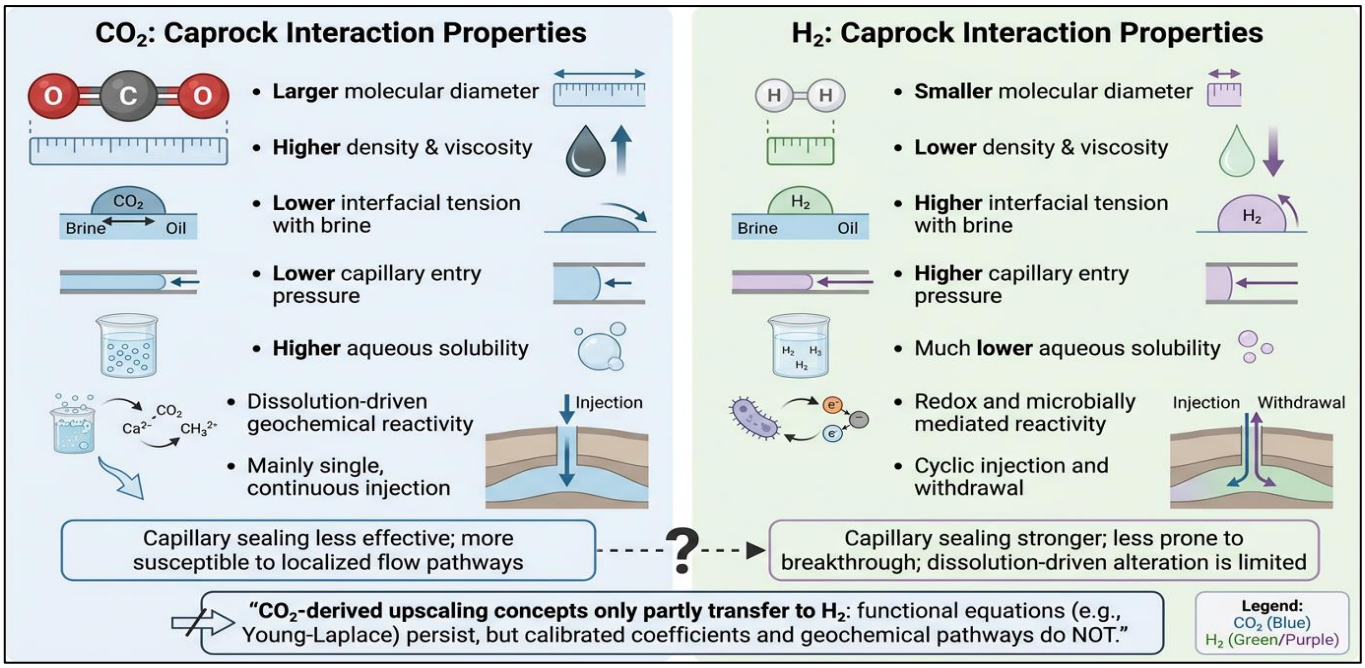

Fig 4 Contrasting Physical Properties Governing CO_2 Versus H_2 Caprock Interaction, and the Resulting Transferability of CO2-Derived Upscaling Concepts to H2 Storage.

The practical consequence is that CO_2-derived quantitative relationships, capillary entry pressure correlations fitted to CO_2-brine-rock contact angle data, and porosity-permeability closures calibrated against CO_2-brine reaction experiments, transfer to H_2 only partially and only where the underlying physics is shared (the Young-Laplace functional form itself, for instance) rather than where the calibrated coefficients are shared. Reporting a small net bulk-scale change for both gases, as the reviewed reservoir-scale literature does (Section 7), is not evidence that the two systems are physically equivalent; it may equally reflect that both sets of reviewed studies happened to model conditions distant from the parameter regimes, high Da, high capillary number, cyclic mechanical loading, where the two gases' divergent properties would matter most.

IV. EVIDENCE SYNTHESIS

➢ *Pore- and Core-Scale Evidence*

Table 1 Verified Pore- and Core-Scale Hydromechanical Degradation Evidence.

Study	Lithology	Fluid	Scale	Method	P, T, salinity	Duration	k before→after	Main finding
Noiriel et al. [4]	Limestone	Acidic water	Core, micro-CT	X-ray micro-CT + hydraulic test	NR	NR	NR (qualitative coupling reported)	Hydraulic property directly coupled to pore microgeometry evolution

ISSN No:-2456-2165 https://doi.org/10.38124/ijisrt/26aug944

Noiriel et al. [5]	Limestone	Reactive brine	Pore/core	Experiment + model	NR	NR	NR	Reactive surface area evolves non-linearly, departs from geometric scaling
Luquot & Gouze [6]	Carbonate	CO_2-brine	Core-flood	Experiment	Multiple, varied	NR	Order-of-magnitude increase (regime-dependent)	Porosity/permeability change strongly flow-regime dependent
Smith et al. [7]	Shale/evaporite (Gothic, Marine Tuscaloosa)	CO_2-brine	Core	XRD, BET	160°C, 15 MPa	~45 days (~35 d Ar control)	NR (mineralogy-dependent, both directions reported)	Clay swelling can offset or reverse dissolution-driven porosity gain

NR = not reported in the verified source. Where a variable was not reported, it is left NR rather than estimated, following the reference-integrity standard applied throughout this review.

➢ *Reservoir-Scale Upscaling Evidence and the Small-Change Claim*

Table 2 Summary of the three Verified Studies that Attempted Upscaling Against an Actual Site.

Study	**Gas / site**	**Upscaling method**	**Duration**	**Reported net change**	**Validation basis**
Wang et al. [8]	CO_2, Plant Daniel (USA)	Core-scale-informed reservoir model, empirical rate constants	130 yr (simulated)	+3.0% reservoir k; −0.9% caprock k	Core-scale experimental data + core-scale simulation, not independent field observation
Adu-Gyamfi et al. [9]	CO_2, Farnsworth (USA)	Coupled hydro-geochemical + hydro-geomechanical reservoir model	Field operational period	~3.3% CO_2-caprock interaction; +1.4% porosity; ~4% permeability	Field-tuned inverted 5-spot model; Mohr-Coulomb failure check
Hashemi & Sedaee [10]	H_2, modelled shale caprocks	Reservoir-scale geochemical numerical simulation	30 yr (simulated)	<1% mineral dissolution, all tested minerals	Numerical only; no field or independent experimental validation reported

Treating these three studies as evidence for a general 'small reservoir-scale change' conclusion would overstate what they demonstrate. Each is a simulation constrained by calibration choices, assumed homogeneous constitutive relationships, and, in two of three cases, no independent field validation of the caprock-scale prediction specifically. The small reported net change could reflect a genuine physical outcome, mineral buffering at reservoir scale as Wang et al. [8] argue directly, or it could reflect coarse discretization and constitutive smoothing that would not capture a wormholed pathway occupying a small fraction of a grid block's volume, unresolved fractures absent from all three models, or simulated durations and flow regimes that did not happen to fall within the high-Da, high-Pe window where pore-scale wormholing is most pronounced (Section 4). The reviewed studies do not themselves distinguish between these explanations, and this review does not either; Section 7.1's pore-scale evidence is drawn predominantly from carbonate lithologies while Section 7.2's reservoir-scale evidence is drawn from shale and mudstone caprocks, a lithology mismatch that further limits how directly the two evidence bases can be compared.

ISSN No:-2456-2165 https://doi.org/10.38124/ijisrt/26aug944

➢ *Cross-Scale Uncertainty Propagation*

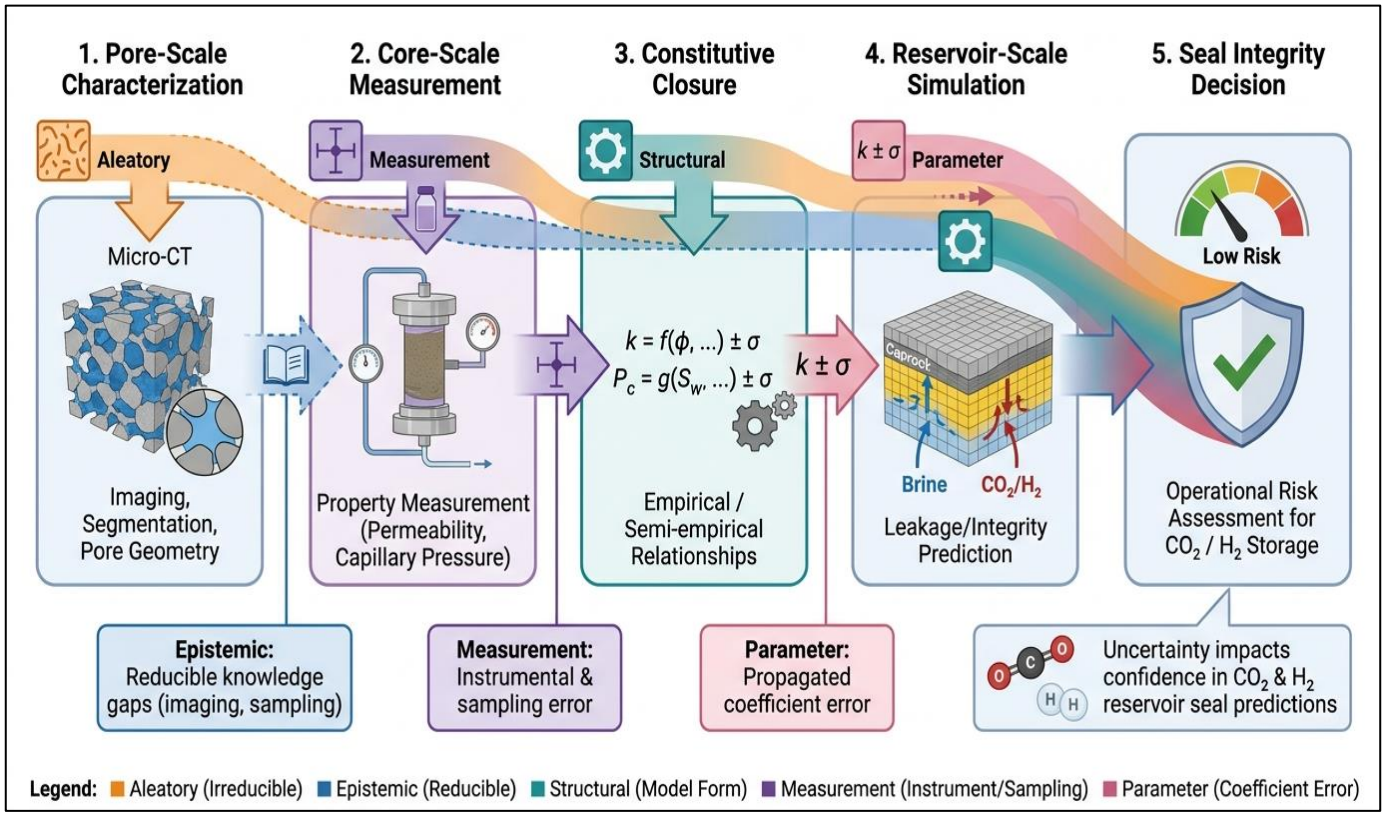

Fig 5 Uncertainty Propagation Cascade from Pore-Scale Characterization to Reservoir-Scale Seal-Integrity Prediction, Grouped by Uncertainty Category.

Five distinct uncertainty categories accumulate across the pore-to-reservoir chain, and treating them as one undifferentiated quantity obscures which are tractable to reduce and which are not. Aleatory uncertainty is genuine physical variability, the real, irreducible heterogeneity of pore geometry, mineralogy, and stress state within a caprock formation, and no amount of additional characterization removes it, only better resolves its spatial structure. Epistemic uncertainty arises from incomplete knowledge rather than physical variability: imaging resolution, segmentation algorithm choice, and operator judgment at the characterization stage are epistemic in this sense, since a different, more capable measurement would reduce them without the rock itself changing [35]. Structural uncertainty is a property of the model form rather than its parameters; the choice between a power-law and an exponential porosity-permeability closure (Section 3.4) is a structural choice that changes predicted behaviour even when both forms are fitted to the same calibration data. Measurement uncertainty is the direct instrumental and sampling error attached to any single reported value, most visible in this review in the NR entries of Table 1 where a variable was simply not measured. Parameter uncertainty, finally, is the familiar propagated error in a fitted coefficient, of the kind a formal sensitivity analysis is built to quantify.

These categories map unevenly onto the reservoir-scale evidence synthesized in Section 7. Imaging and segmentation uncertainty, predominantly epistemic, is the most directly quantifiable in principle, through repeat scans, alternative segmentation algorithms applied to the same raw data, and comparison against independent measurement, though none of the studies verified in this review report having done so. REV and scale uncertainty combine aleatory heterogeneity with epistemic uncertainty about whether the chosen domain satisfies the transport REV (Section 5); it is quantifiable through the convergence-testing approach reviewed there but is rarely reported for caprock-specific studies at present. Structural uncertainty in constitutive closure choice is the least well constrained of the five categories in the literature reviewed here: none of the three reservoir-scale upscaling studies in Table 2 reported a sensitivity analysis across alternative closure relationships, formal global sensitivity analysis, Monte Carlo parameter sampling, or a polynomial-chaos or Bayesian surrogate of the kind used to propagate structural and parameter uncertainty jointly in adjacent subsurface-Modeling fields, which means the small net-change figures reported in Table 2 carry an unquantified structural-uncertainty component in addition to their stated or implied parameter uncertainty. This is not a criticism of the individual studies, whose stated scope did not include uncertainty quantification, but it does mean the confidence with which this review's own Section 7.2 finding can be held is itself bounded by an uncertainty category that the underlying evidence base does not yet let us quantify.

ISSN No:-2456-2165 https://doi.org/10.38124/ijisrt/26aug944

➢ *Toward a Physics-Consistent Pore-to-Reservoir Workflow*

- *Proposed Workflow*

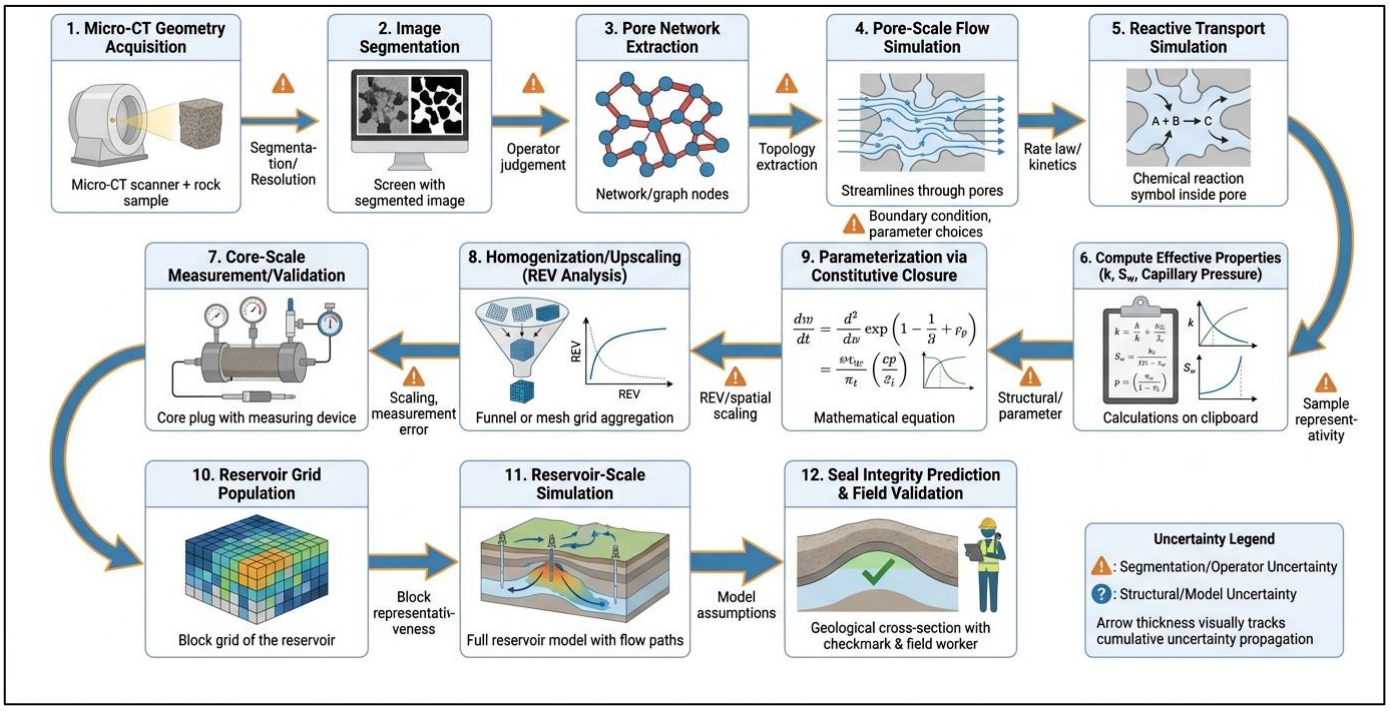

Fig 6 Proposed Physics-Consistent Workflow for Pore-to-Reservoir-Scale Caprock Assessment. This is a Proposed Conceptual Structure, not a Claim that Any Single Published Study has Executed all Twelve Steps in Sequence.

No study reviewed here executes this full sequence against a single site with a single, internally consistent set of samples; Wang et al. [8] and Adu-Gyamfi et al. [9] approximate steps 1 through 9 and 10 for CO_2, without step 11 field validation of the caprock-specific prediction, and no reviewed H_2 study approximates more than steps 9 through 10 alone. The workflow is proposed as a target structure against which future studies, and future reviews of this kind, can be assessed, not as a demonstrated achievement of the current literature.

- *Comparing Upscaling Methods*

Direct numerical upscaling (solving governing equations on the full segmented geometry) preserves the most pore-scale information but is computationally intractable beyond core scale. Volume averaging and homogenization theory provide a mathematically principled route to effective parameters but require an REV to exist (Section 5) and generally assume periodicity or statistical stationarity that heterogeneous caprock may not satisfy. Pore-network-derived effective properties are computationally cheaper than direct simulation but depend on how accurately the network extraction (Section 3.2) represents the true pore topology. Empirical porosity-permeability laws, the closure form used in Section 3.4, are the most commonly applied in reservoir-scale caprock studies specifically because they require no pore-scale simulation at all, at the cost of being fitted rather than derived and therefore not necessarily transferable outside the calibration conditions [17]. Multiscale finite-element approaches solve coupled cell problems on an REV to compute a full, potentially anisotropic permeability tensor rather than a scalar closure, a more rigorous but more computationally demanding alternative [34].

- *Machine Learning as a Prospective, Not Present, Contribution*

Machine learning applications to pore-scale and upscaling problems fall into three methodological families that this review's earlier drafts did not adequately distinguish. Convolutional neural networks (CNNs) trained directly on segmented pore geometry images predict permeability substantially faster than direct simulation once trained, with reported accuracy that has improved considerably since the earliest demonstrations [28]; a systematic review of deep learning applied to pore-scale imaging and Modeling more broadly, spanning segmentation, property prediction, and multiphase flow, is available and is the single most comprehensive entry point into this literature for the specific problem this review addresses [29]. Graph neural networks (GNNs), which represent the pore network itself, pores as nodes, throats as edges, as the model's native data structure rather than a voxel grid, have been combined with CNNs in hybrid architectures reporting comparable accuracy to standalone CNNs at substantially lower parameter count [30]. Physics-informed machine learning, in which a network is trained to satisfy governing PDE constraints rather than fit data alone, was formalized by Raissi et al. [25] and reviewed comprehensively by Karniadakis et al. [26]; within subsurface flow specifically, PINNs have been applied both to learning parameters and constitutive relationships directly from flow data [27] and, more directly relevant to this review's central problem, to permeability upscaling itself,

ISSN No:-2456-2165 https://doi.org/10.38124/ijisrt/26aug944

where a PINN incorporating an analytical Darcy-Ohm-law solution demonstrated accurate upscaling across multiple aggregation levels for previously unseen digital rock samples [31].

None of these three families has been demonstrated for the caprock-specific, reactive, multiphase problem this review addresses; the CNN, GNN, and PINN studies just cited train and validate on single-phase permeability prediction for sandstone or generic porous media, not on reactive dissolution, capillary sealing, or coupled hydromechanical caprock behaviour (Table 3). The specific limitation most relevant to this review's problem is out-of-distribution generalization: a network trained on pore topologies from one lithology or one segmentation protocol has no guaranteed accuracy when applied to a topologically distinct pore network, for example a fractured caprock outside the training distribution, a concern that follows directly from Section 5's finding that an REV, and by extension a representative training set, may not exist for structurally heterogeneous caprock. This specific failure mode has not, to our knowledge, been tested for caprock pore-network topologies in any study reviewed here; we identify this as an open methodological question rather than attach a citation that does not yet exist to support it. Where machine learning could prospectively contribute, based on its demonstrated role in the adjacent single-phase permeability-prediction and subsurface-flow applications cited above, is in parameterizing sub-grid heterogeneity effects (Section 5) that current empirical closures do not capture, propagating uncertainty (Section 8) more efficiently than repeated forward simulation, and connecting high-resolution digital rock output directly to continuum solvers without the intermediate, information-lossy step of fitting a single closure relation; realizing that potential would itself require first resolving the out-of-distribution problem just described, and extending validation from single-phase permeability to the reactive, multiphase, hydromechanically coupled problem this review addresses, neither of which is a minor implementation detail.

Table 3 Machine Learning Approaches Applied to Pore-Scale Property Prediction and Upscaling: Verified Scope and Demonstrated Maturity for this Review's Problem.

Method	**Physics included**	**Demonstrated task**	**Validated on caprock/reactive systems?**
CNN [28,29,30]	None (data-driven image-to-property mapping)	Single-phase permeability prediction from segmented images	No – sandstone/generic porous media only
GNN (hybrid with CNN) [30]	None (graph-structured, topology-aware)	Permeability prediction at lower parameter count than CNN alone	No – same evidence base as CNN
PINN [25,26,27,31]	Governing PDE constraints embedded in training	Parameter/constitutive learning [27]; permeability upscaling across aggregation levels [31]	No – single-phase, non-reactive systems only

V. DISCUSSIONS

➢ *Demonstrated Mechanisms Versus Hypothesis*

Directly demonstrated by the evidence reviewed: regime-dependent dissolution patterning (face dissolution, wormholing, uniform dissolution) as a function of flow rate, in carbonate systems [6,10]; non-linear evolution of reactive surface area during dissolution [5]; clay-swelling-driven porosity change that can oppose dissolution-driven porosity gain in evaporite/shale caprock specifically [7]; and small net reservoir-scale permeability and mineral-alteration change in the three site-specific studies reviewed [8,9,10]. Presented here as plausible but not directly demonstrated by any single cited study: that reservoir-scale mineral buffering, sub-grid averaging, and flow-regime placement outside the wormholing-prone window jointly explain the pore-to-reservoir discrepancy (Section 7.2); that the same regime-dependent dissolution pattern documented in carbonate systems applies quantitatively, rather than only qualitatively, to shale and mudstone caprock; and that CO2-derived porosity-permeability closures retain quantitative validity for H2 systems given the physical property divergence documented in Section 6.

➢ *Environmental Safety Implications*

The three site-specific reservoir-scale studies reviewed report outcomes consistent with continued caprock integrity under the specific conditions each modelled. This is a bounded, site-specific finding, not a general property of caprock behaviour under CO_2 or H_2 storage, and the mechanisms reviewed in Sections 5 and 6, flow-regime dependence and REV-scale information loss specifically, identify concrete physical conditions under which a different outcome would be expected. A safety assessment relying on pore-scale dissolution-rate parameters transferred directly to reservoir scale without an explicit upscaling step, of the kind reviewed critically in Section 9.2, would not be well supported by the evidence synthesized here. Independent field-scale pressure and geomechanical monitoring at operating CO_2 storage sites, direct pressure measurement at Sleipner [12] and geomechanical monitoring at In Salah [13], together with a comparative analysis of surface deformation across Sleipner, Weyburn, and In Salah [15], have not indicated caprock behaviour approaching failure thresholds; these are independent, site-specific field observations rather than validation of the pore-to-reservoir upscaling studies in Table 5, but they are broadly consistent in direction.

ISSN No:-2456-2165 https://doi.org/10.38124/ijisrt/26aug944

➢ *Relation to Prior Reviews*

This review's contribution relative to prior digital-rock-physics and reservoir-scale caprock reviews is the explicit treatment of the transition between them as the primary object of study, formalized through the input-transformation-output-uncertainty structure in Section 2 and the twelve-step workflow in Section 9.1, together with the explicit separation of CO_2 and H_2 physics (Section 6) before any comparison of their reservoir-scale outcomes is drawn.

➢ *Critical Research Agenda*

- Paired before/after micro-CT experiments on identical samples, imaged, reacted, and re-imaged with registration-corrected comparison, specifically for shale and mudstone caprock lithologies rather than the carbonate systems that dominate the current pore-scale wormholing literature.
- Dynamic (time-resolved) imaging of reactive flow, rather than end-point before/after comparison, to directly observe wormhole initiation and growth rather than infer it from final-state porosity fields.
- Identical samples characterized across scales, pore-network model, core-flood experiment, and, where feasible, field-scale monitoring at the same site, to test the upscaling chain directly rather than by comparison across unrelated studies as this review has necessarily done.
- Coupled geochemical-geomechanical experiments applying reactive flow and effective-stress change simultaneously, since Section 3.4 identifies that the two mechanisms are reviewed here only as parallel, not coupled, processes in the existing literature.
- Capillary entry-pressure measurement under UHS-relevant cyclic pressure conditions specifically, extending single-cycle measurements of the kind reviewed in Section 3.3 [19] to repeated injection-withdrawal cycling.
- Fracture-containing caprock samples and models, since all pore-scale and reservoir-scale studies reviewed here assume an unfractured or effectively continuum caprock, a simplification Section 5 identifies as a specific limit on REV existence.
- Multiscale benchmark datasets, publicly archived, pairing raw micro-CT data with reservoir-scale model input and output for the same site, that would allow future reviews of this kind to test upscaling claims quantitatively rather than qualitatively as done here.
- Uncertainty-aware upscaling that reports a structural-uncertainty sensitivity analysis across alternative closure relationships (Section 8), which none of the three reservoir-scale studies reviewed here provided.

VI. CONCLUSION

The evidence reviewed supports a specific, bounded statement: at the small number of sites where the pore-to-reservoir upscaling chain has been examined, net caprock change is small relative to pore-scale evidence alone, for both CO_2 and, on more limited H_2 evidence, H_2 storage. This does not establish, and this review does not claim, that pore-scale wormholing evidence and reservoir-scale small-change evidence have been reconciled; the mechanisms that could explain the apparent discrepancy, evaluated in Sections 5, 6, and 8.2, remain distinguishable candidates rather than an established explanation. The twelve-step workflow proposed in Section 9.1 and the input-transformation-output-uncertainty framework in Section 2 are offered as a structure against which that reconciliation can be pursued directly, through the specific paired, multiscale, uncertainty-reporting studies identified in Section 11, rather than inferred from separately conducted pore-scale and reservoir-scale literatures as the field currently must.

➢ *Declaration of Competing Interests*

The author declares no known competing financial interests or personal relationships that could have appeared to influence the work reported in this paper.

➢ *Funding*

This work received no external funding.

➢ *Data Availability*

This is a review synthesizing previously published data. All quantitative findings reported in Section 7 are drawn directly from cited primary sources, with unreported variables flagged NR rather than estimated; no new experimental or simulation data were generated for this review.

REFERENCES

[1]. Blunt MJ. Flow in porous media - pore-network models and multiphase flow. Curr Opin Colloid Interface Sci. 2001;6(3):197-207.
[2]. Middleton RS, Keating GN, Stauffer PH, et al. The cross-scale science of CO2 capture and storage: from pore scale to regional scale. Energy Environ Sci. 2012;5(6):7328-7345.
[3]. Meakin P, Tartakovsky AM. Modeling and simulation of pore-scale multiphase fluid flow and reactive transport in fractured and porous media. Rev Geophys. 2009;47:RG3002.
[4]. Noiriel C, Bernard D, Gouze P, Thibault X. Hydraulic properties and microgeometry evolution accompanying limestone dissolution by acidic water. Oil Gas Sci Technol. 2005;60:177-192.
[5]. Noiriel C, Luquot L, Made B, Raimbault L, Gouze P, van der Lee J. Changes in reactive surface area during limestone dissolution: an experimental and Modeling study. Chem Geol. 2009;265:160-170.
[6]. Luquot L, Gouze P. Experimental determination of porosity and permeability changes induced by injection of CO2 into carbonate rocks. Chem Geol. 2009;265:148-159.
[7]. Smith MM, Sholokhova Y, Hao Y, Carroll SA. Evaporite caprock integrity: an experimental study of reactive mineralogy and pore-scale heterogeneity during brine-CO2 exposure. Environ Sci Technol. 2013;47:262-268.
[8]. Wang Y, Zhang L, Soong Y, Dilmore R, Lei H, Li X. From core-scale experiment to reservoir-scale modeling: a scale-up approach to investigate reaction-

ISSN No:-2456-2165 https://doi.org/10.38124/ijisrt/26aug944

induced permeability evolution of CO2 storage reservoir and caprock at a U.S. CO2 storage site. Comput Geosci. 2019. doi:10.1016/j.cageo.2019.01.006.

[9]. Adu-Gyamfi B, Ampomah W, Tu J, Sun Q, Erzuah S, Acheampong S. Assessment of chemo-mechanical impacts of CO2 sequestration on the caprock formation in Farnsworth oil field, Texas. Sci Rep. 2022. doi:10.1038/s41598-022-16990-x.

[10]. Hashemi M, Sedaee B. Understanding caprock integrity in underground hydrogen storage: a geochemical study of mineral alteration and sealing efficiency. Int J Hydrogen Energy. 2025;154:150300.

[11]. Morais S, Cario A, Liu N, Bernard D, Lecoutre C, Garrabos Y, et al. Studying key processes related to CO2 underground storage at the pore scale using high pressure micromodels. React Chem Eng. 2020;5:1156-1185.

[12]. Chadwick RA, Williams GA, Williams JDO, Noy DJ. Measuring pressure performance of a large saline aquifer during industrial-scale CO2 injection: the Utsira Sand, Norwegian North Sea. Int J Greenh Gas Control. 2012;10:374-388.

[13]. White JA, Chiaramonte L, Ezzedine S, Foxall W, Hao Y, Ramirez A, McNab W. Geomechanical behavior of the reservoir and caprock system at the In Salah CO2 storage project. Proc Natl Acad Sci USA. 2014;111:8747-8752.

[14]. Biot MA. General theory of three-dimensional consolidation. J Appl Phys. 1941;12(2):155-164.

[15]. Verdon JP, Kendall JM, Stork AL, Chadwick RA, White DJ, Bissell RC. Comparison of geomechanical deformation induced by megatonne-scale CO2 storage at Sleipner, Weyburn, and In Salah. Proc Natl Acad Sci USA. 2013;110:E2762-E2771.

[16]. Bear J. Dynamics of Fluids in Porous Media. New York: American Elsevier; 1972.

[17]. Hommel J, Coltman E, Class H. Porosity-permeability relations for evolving pore space: a review with a focus on (bio-)geochemically altered porous media. Transp Porous Media. 2018;124(2):589-629.

[18]. Baqer Y, Chen X. A review on reactive transport model and porosity evolution in the porous media. Environ Sci Pollut Res. 2022. doi:10.1007/s11356-022-20466-w.

[19]. Alanazi A, Ali M, Mowafi M, Bawazeer S, Kaidar ZK, Hoteit H. Capillary-sealing efficiency of mica-proxy caprock for CO2/H2 geologic storage in the presence of organic acids and nanofluids. SPE J. 2023;28(6):3308-3323.

[20]. Heinemann N, Alcalde J, Miocic JM, Hangx SJT, Kallmeyer J, Ostertag-Henning C, Hassanpouryouzband A, et al. Enabling large-scale hydrogen storage in porous media - the scientific challenges. Energy Environ Sci. 2021;14(2):853-864.

[21]. Thaysen EM, McMahon S, Strobel GJ, Butler IB, Ngwenya BT, Heinemann N, Wilkinson M, Hassanpouryouzband A, McDermott CI, Edlmann K. Estimating microbial growth and hydrogen consumption in hydrogen storage in porous media. Renew Sustain Energy Rev. 2021;151:111481.

[22]. Iglauer S, Pentland CH, Busch A. CO2 wettability of seal and reservoir rocks and the implications for carbon geo-sequestration. Water Resour Res. 2015;51:729-774.

[23]. Edlmann K, Hinchliffe S, Heinemann N, Johnson G, Ennis-King J, McDermott CI. Cyclic CO2-H2O injection and residual trapping: implications for CO2 injection efficiency and storage security. Int J Greenh Gas Control. 2019;80:1-9.

[24]. Jackson SJ, Lin Q, Krevor S. Representative elementary volumes, hysteresis, and heterogeneity in multiphase flow from the pore to continuum scale. Water Resour Res. 2020;56(6):e2019WR026396.

[25]. Raissi M, Perdikaris P, Karniadakis GE. Physics-informed neural networks: a deep learning framework for solving forward and inverse problems involving nonlinear partial differential equations. J Comput Phys. 2019;378:686-707.

[26]. Karniadakis GE, Kevrekidis IG, Lu L, Perdikaris P, Wang S, Yang L. Physics-informed machine learning. Nat Rev Phys. 2021;3(6):422-440.

[27]. Tartakovsky AM, Marrero CO, Perdikaris P, Tartakovsky GD, Barajas-Solano D. Physics-informed deep neural networks for learning parameters and constitutive relationships in subsurface flow problems. Water Resour Res. 2020;56(5):e2019WR026731.

[28]. Wu J, Yin X, Xiao H. Seeing permeability from images: fast prediction with convolutional neural networks. Sci Bull. 2018;63(18):1215-1222.

[29]. Wang YD, Blunt MJ, Armstrong RT, Mostaghimi P. Deep learning in pore scale imaging and modeling. Earth Sci Rev. 2021;215:103555.

[30]. Zhai S, Geng S, Li C, Ye J, Tang D, Zhang D. An improved convolutional neural network for predicting porous media permeability from rock thin sections. Gas Sci Eng. 2024;127:205365.

[31]. Elmorsy M, El-Dakhakhni W, Coulibaly P. Rapid permeability upscaling of digital porous media via physics-informed neural networks. Water Resour Res. 2023;59(12):e2023WR035064.

[32]. Wang Y, Chakrapani TH, Wen Z, Hajibeygi H. Pore-scale simulation of H2-brine system relevant for underground hydrogen storage: a lattice Boltzmann investigation. Adv Water Resour. 2024;190:104756.

[33]. McClure JE, Fan M, Berg S, Armstrong RT, Berg CF, Li Z, Ramstad T. Derivation of a representative elementary volume for upscaled two-phase flow in porous media. Technical report, Oak Ridge National Laboratory.

[34]. Schulz R, Ray N, Zech S, Rupp A, Knabner P. Beyond Kozeny-Carman: predicting the permeability in porous media. Transp Porous Media. 2019;130:487-512.

[35]. Der Kiureghian A, Ditlevsen O. Aleatory or epistemic? Does it matter? Struct Saf. 2009;31(2):105-112.

[36]. Azizmohammadi S, Matthäi SK. Is the permeability of naturally fractured rocks scale dependent? Water Resour Res. 2017;53(10):8041-8063.